Collision dynamics of skyrmions in a two-component Bose-Einstein condensate

Tomoya Kaneda and Hiroki Saito

Department of Engineering Science, University of Electro-Communications, Tokyo 182-8585, Japan

(Received 8 January 2016; published 4 March 2016)

The dynamics of skyrmions in a two-component Bose-Einstein condensate is numerically investigated in the mean-field theory. When two skyrmions collide with each other, they are first united and then scattered into various states. For head-on collisions, skyrmions with unit winding number are scattered. The collision dynamics with an impact parameter are shown to depend on the relative phase. These dynamic processes are characterized by integer winding numbers.

DOI: 10.1103/PhysRevA.93.033611

I. INTRODUCTION

A quantized vortex in a superfluid is a topological excitation that reflects the U(1) manifold of the order-parameter space. For multicomponent superfluids with larger degrees of freedom in the order-parameter space, there exists a rich variety of topological excitations, such as spin vortices, monopoles, and skyrmions [1], which have been realized in superconductors [2,3], superfluid ^{3}He [4], Bose-Einstein condensates (BECs) of ultracold gases [5–9], and exciton-polariton superfluids [10,11].

When two or more topological excitations are generated in proximity to each other, they can exhibit interesting dynamics. The simplest example is a quantized vortex-antivortex pair (called a vortex dipole), which travels at a constant velocity in a uniform system. Such a topological object in a BEC has been studied theoretically [12,13] and realized experimentally [14–17]. A pair of quantized vortices with the same circulation rotate around one another [18,19]. When two quantized vortex lines approach each other, they interact with one another [20], and a reconnection occurs [21,22]. Two copropagating quantized vortex rings show leapfrogging dynamics [23,24], such as those in classical fluids, and when they collide with each other, they merge and split again into vortex rings [24,25]. For multicomponent or spinor BECs, interaction between half-quantum vortices [26], reconnection of 1/3 vortices [27], the dynamics of spin-vortex dipoles [28], and generation of multiple skyrmions [29] have been predicted. Recently, the collision of half-quantum vortices in a spin-1 BEC was observed [30].

In the present paper, we investigate the collision and scattering dynamics of skyrmions in a two-component BEC. Although the scattering of skyrmions has been studied in the context of high-energy physics [31–33], previous studies on skyrmions in a two-component BEC have mainly focused on their static properties [34–40]. A skyrmion in a two-component BEC consists of a quantized vortex ring in one component, whose core is occupied by a quantized vortex of the other component. A skyrmion therefore travels at a constant velocity, since a vortex ring has a momentum along the symmetry axis. Let us consider a situation in which two skyrmions move toward and collide with each other. The topology of a skyrmion is characterized by an integer winding number, and the sum of the winding numbers of the two skyrmions, $W_1 + W_2$, is conserved during their collision, if the wave functions are always restricted to the SU(2) manifold. When the winding number is conserved, we find that $W_1 + W_2$ skyrmions with unit winding number are scattered after the collision. We present the collision dynamics of skyrmions with various winding numbers. For off-axis collisions with finite impact parameters, we show that the dynamics depends on the relative phases between the two skyrmions, whereas the head-on collisions are independent of the relative phases.

This paper is organized as follows. Section II introduces a skyrmion in a two-component BEC and discusses the problem that we consider in this paper. Section III shows numerical results for the dynamics of skyrmions. Section IV presents our conclusions for this study.

II. FORMULATION OF THE PROBLEM

A. Skyrmion in a two-component BEC

First, we briefly review a skyrmion in a two-component BEC. The mean-field energy of a two-component BEC in a three-dimensional (3D) free space is given by

$$E = \int d\boldsymbol{r} \left(- \sum_{j=1}^{2} \psi_j^* \frac{\hbar^2}{2m_j} \nabla^2 \psi_j + \sum_{j,j'} \frac{g_{jj'}}{2} |\psi_j|^2 |\psi_{j'}|^2 \right), \tag{1}$$

where ψ_j and m_j are the macroscopic wave function and the mass of the atom of the jth component, respectively. The interaction coefficient in Eq. (1) is defined as $g_{jj'} = 2\pi\hbar^2 a_{jj'}(m_j^{-1} + m_{j'}^{-1})$, where $a_{jj'} = a_{j'j}$ is the s-wave scattering length between the atoms in components j and j'.

When $g_{11} \simeq g_{22} \simeq g_{12}$ and the interaction energy is much larger than the kinetic energy, the total density $\rho = |\psi_1|^2 + |\psi_2|^2$ is approximately uniform. The wave functions are then written as

$$\boldsymbol{\Psi}(\boldsymbol{r}) = \begin{pmatrix} \psi_1(\boldsymbol{r}) \\ \psi_2(\boldsymbol{r}) \end{pmatrix} = \sqrt{\rho} \begin{pmatrix} \xi_1(\boldsymbol{r}) \\ \xi_2(\boldsymbol{r}) \end{pmatrix}, \tag{2}$$

where $|\xi_1|^2 + |\xi_2|^2 = 1$. The two-component state is thus described by the SU(2) manifold. A skyrmion is defined as a topological state in which $\Psi(\boldsymbol{r})$ goes to the same state Ψ_0 at infinity, i.e., $\lim_{r\to\infty} \Psi(\boldsymbol{r}) = \Psi_0$. Such a state can be described by a map of SU(2) on the sphere S^3 in four-dimensional (4D) space. (This can be understood from a lower-dimensional analogy, e.g., a map of SU(2) on the sphere S^2 in 3D space: imagine that the sphere is cut open from a point on the sphere, and the cut edge is expanded to infinity; this is equivalent to a two-dimensional (2D) plane satisfying $\lim_{r\to\infty} \Psi(\boldsymbol{r}) = \Psi_0$.)

Topologically, the way in which SU(2) is mapped onto S^3 is expressed by $\pi_3(\mathrm{SU}(2)) = \mathbb{Z}$, which indicates that the skyrmion state is characterized by an integer topological number.

Separating the complex variables ξ_j in Eq. (2) into their real and imaginary parts, $\xi_j = c_j + i d_j$, we have $|\xi_1|^2 + |\xi_2|^2 = c_1^2 + d_1^2 + c_2^2 + d_2^2 = 1$, which is a unit sphere in four dimensions. Using polar coordinates as $c_1 = \sin\alpha \sin\beta \sin\gamma$, $d_1 = \sin\alpha \sin\beta \cos\gamma$, $d_2 = \sin\alpha \cos\beta$, and $c_2 = \cos\alpha$, Eq. (2) becomes

$$\boldsymbol{\Psi}(\boldsymbol{r}) = \sqrt{\rho}\begin{pmatrix} i\sin\alpha(\boldsymbol{r})\sin\beta(\boldsymbol{r})e^{-i\gamma(\boldsymbol{r})} \\ \cos\alpha(\boldsymbol{r}) + i\sin\alpha(\boldsymbol{r})\cos\beta(\boldsymbol{r}) \end{pmatrix}. \tag{3}$$

Noting that the area of the unit sphere in four dimensions is $\int_0^\pi d\alpha \int_0^\pi d\beta \int_0^{2\pi} d\gamma \sin^2\alpha \sin\beta = 2\pi^2$, the number of times that S^3 (3D space) covers SU(2) (two-component state) is expressed as

$$W = \frac{1}{2\pi^2}\int d\boldsymbol{r} \sin^2\alpha(\boldsymbol{r})\sin\beta(\boldsymbol{r})\det\left(\frac{\partial(\alpha,\beta,\gamma)}{\partial(x,y,z)}\right), \tag{4}$$

where $\det(\cdots)$ is the Jacobian. The winding number W is an integer reflecting $\pi_3(\mathrm{SU}(2)) = \mathbb{Z}$. In the numerical analysis, it is convenient to express the two-component state as

$$\boldsymbol{\Psi}(\boldsymbol{r}) = \sqrt{\rho}\begin{pmatrix} \cos\frac{\theta(\boldsymbol{r})}{2}e^{i\phi_1(\boldsymbol{r})} \\ \sin\frac{\theta(\boldsymbol{r})}{2}e^{i\phi_2(\boldsymbol{r})} \end{pmatrix}. \tag{5}$$

Since the area of the unit sphere $c_1^2 + d_1^2 + c_2^2 + d_2^2 = 1$ is written as $\int_0^\pi d\theta \int_0^{2\pi} d\phi_1 \int_0^{2\pi} d\phi_2 \frac{1}{4}\sin\theta = 2\pi^2$, the winding number W is given by

$$W = \frac{1}{8\pi^2}\int d\boldsymbol{r} \sin\theta(\boldsymbol{r})\det\left(\frac{\partial(\theta,\phi_1,\phi_2)}{\partial(x,y,z)}\right), \tag{6}$$

which is also an integer.

B. Dynamics of the system

In the mean-field approximation, the dynamics of the two-component BEC is described by the Gross-Pitaevskii (GP) equation,

$$i\hbar\frac{\partial\psi_1}{\partial t} = -\frac{\hbar^2}{2m_1}\nabla^2\psi_1 + g_{11}|\psi_1|^2\psi_1 + g_{12}|\psi_2|^2\psi_1, \tag{7a}$$

$$i\hbar\frac{\partial\psi_2}{\partial t} = -\frac{\hbar^2}{2m_2}\nabla^2\psi_2 + g_{22}|\psi_2|^2\psi_2 + g_{12}|\psi_1|^2\psi_2. \tag{7b}$$

In the following, we assume $m_1 = m_2 \equiv m$ and $g_{11} = g_{22} = g_{12} \equiv g$. The characteristic length and velocity of the system are given by the healing length $\xi = \hbar/(mgn_0)^{1/2}$ and sound velocity $v_s = (gn_0/m)^{1/2}$, where n_0 is the uniform density far from the skyrmions. The characteristic time is given by $\tau = \xi/v_s = \hbar/(gn_0)$.

We numerically solve the GP equation using the pseudospectral method. The initial state of a skyrmion is prepared as follows. First we numerically imprint a skyrmion as

$$\psi_1(\boldsymbol{r}) = \sqrt{n_0}e^{-[(\sqrt{\Delta x^2+\Delta y^2}-R_s)^2+\Delta z^2]/r_s^2}e^{in\phi}, \tag{8a}$$

$$\psi_2(\boldsymbol{r}) = \sqrt{n_0 - |\psi_1(\boldsymbol{r})|^2}e^{i\ell\chi}, \tag{8b}$$

where $\Delta\boldsymbol{r} = \boldsymbol{r} - \boldsymbol{r}_0$, and $\boldsymbol{r}_0$ is the center of the skyrmion, R_s and r_s are constants that determine the shape of the skyrmion, n and ℓ are integers, $\phi = \arg(\Delta x + i\Delta y)$, and $\chi = \arg(\sqrt{\Delta x^2 + \Delta y^2} - R_s + i\Delta z) - \arg(\sqrt{\Delta x^2 + \Delta y^2} + R_s + i\Delta z)$. The winding number of the state in Eqs. (8) is $W = n\ell$. We then perform the imaginary-time propagation for some time (typically 20τ), in which i on the left-hand side of Eq. (7) is replaced by -1, and the wave functions are normalized to their initial values in every time step. By the imaginary-time propagation, the excess energy of the skyrmion imprinted by Eqs. (8) is relaxed. Starting from the wave functions obtained by the imaginary-time propagation, we perform the real-time propagation to study the dynamics of the system, where a small initial noise is added to the initial state to break the symmetry. The size of the numerical mesh is typically $(256)^3$ or $(512)^3$. The periodic boundary condition is imposed by the pseudospectral method, which does not affect the dynamics of skyrmions located near the center of the numerical space.

III. NUMERICAL RESULTS

A. Dynamics of a single skyrmion

First we numerically investigate the dynamics of a single skyrmion. The initial state is given by Eqs. (8) with $R_s = 20\xi$, $r_s = 10\xi$, and $n = \ell = 1$. Component 1 has a donut shape with a quantized circulation, which is held by the quantized vortex ring in component 2, as shown in Fig. 1(a). Since the vortex ring in component 2 has a momentum, the skyrmion travels in the $-z$ direction. We find that the shape of the skyrmion remains almost unchanged for a long time [41].

Figure 1(b) shows the time evolution of the position z_s of the skyrmion and its winding number W. The position z_s is defined as the z coordinate of the core of the vortex ring in component 2. From the slope of z_s in Fig. 1(b), the skyrmion is found to travel at a constant velocity $\simeq 0.09 v_s$. For a single-component superfluid, a vortex ring travels at a velocity $v_r \simeq \frac{\hbar}{2R_r m}\ln\frac{8R_r}{r_r}$, where R_r is the radius of a ring and r_r is the size of the vortex core [42]. Substituting R_s and r_s into R_r and r_r, we obtain $v_r \simeq 0.07 v_s$, which is in reasonable agreement with the skyrmion velocity in Fig. 1. The winding number W is calculated using Eq. (6), which is always $\simeq 1$ during the time evolution. The deviation from 1 is less than 1%, which is due to the numerical error from the spatial discretization.

B. Collision dynamics of two skyrmions

We first examine the dynamics of the head-on collision of two skyrmions, where each winding number is $W = 1$, and the total winding number is $W_{\mathrm{tot}} = 1 + 1 = 2$. Figure 2(a) is the initial state, with the isodensity surfaces of component 1 shown. The skyrmions travel toward each other, and a head-on collision occurs at $t \simeq 160\tau$; at this time, the two rings of component 1 touch at two regions [Fig. 2(b)]. When the two rings merge with each other, two quantized vortices are created on the ring [Fig. 2(c)]. The ring is then divided into pieces, and the two quantized vortices on the ring become independent rings, which then become two skyrmions with unit winding number [Fig. 2(d)]. After that, the two small skyrmions are scattered in directions perpendicular to the incident directions.

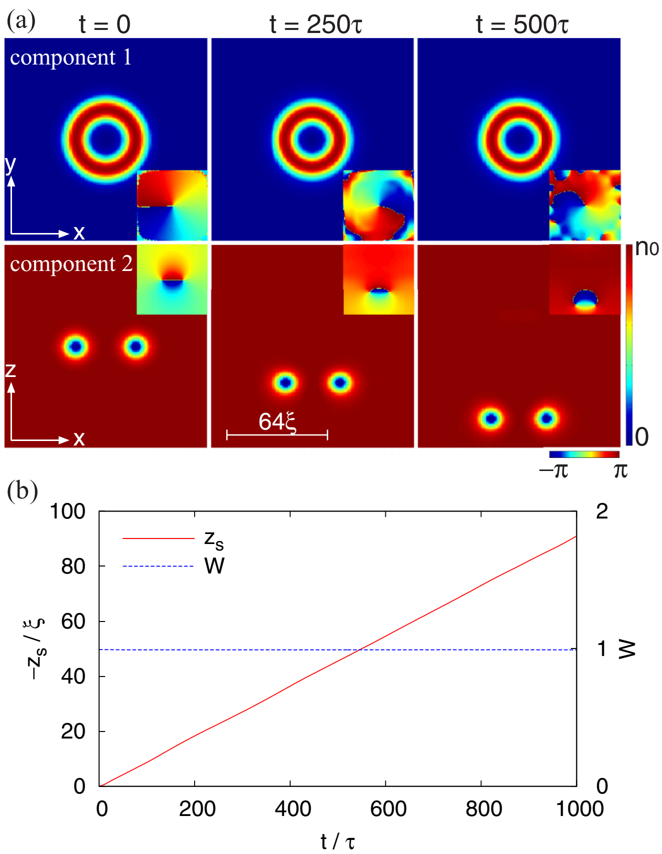

FIG. 1. Dynamics of a single skyrmion. (a) Cross-sectional density profiles of component 1 at $z = z_s$ (upper panels) and those of component 2 at $y = 0$ (lower panels), where z_s is the z coordinate of the position of the vortex-ring core in component 2. The insets show the phase profiles. The field of view is $128\xi \times 128\xi$. (b) Time evolution of z_s (red solid line) and the winding number W (blue dashed line).

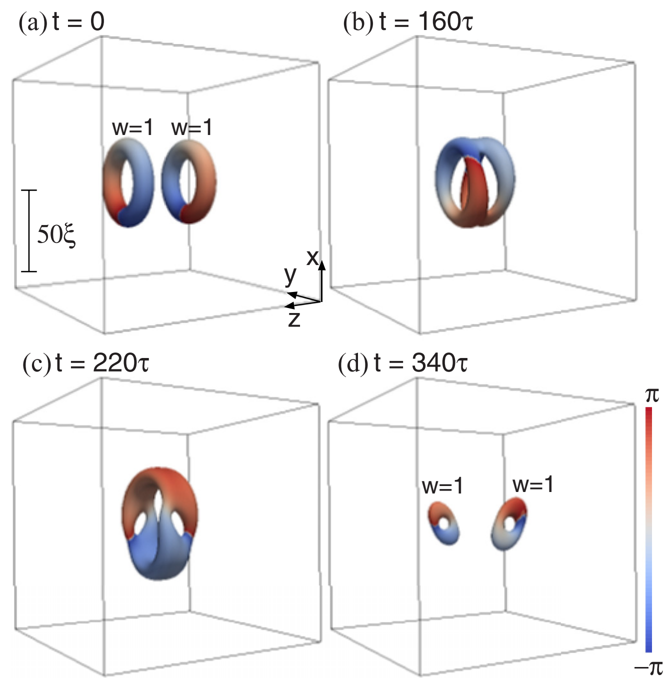

FIG. 2. Dynamics of a collision and scattering of two skyrmions. Isodensity surfaces of component 1 at $|\psi_1|^2 = 0.5n_0$ are shown; the color represents the phase at the surface. Each skyrmion in (a) has a winding number $W = 1$, and the total winding number is $W_{\rm tot} = 2$. The parameters for preparing the initial skyrmions are $R_s = 20\xi$, $r_s = 10\xi$, $\boldsymbol{r}_0 = (0,0,\pm 20\xi)$, $n = \pm 1$, and $\ell = \pm 1$. The size of each box is $(128\xi)^3$. See Ref. [43] for a movie of the dynamics.

The part of component 1 that is not contained in the scattered skyrmions spreads into the surrounding component 2 without topological structure, which has disappeared from Fig. 2(d). In this dynamics, the deviation of the total winding number $W_{\rm tot}$ from the initial value of 2 is less than 1%. The variation in the winding number is due to the roughness of the numerical mesh.

Figure 3 shows the dynamics of a head-on collision of two skyrmions with $W = 2$ ($W_{\rm tot} = 2 + 2 = 4$). The two donuts of component 1 merge to form a multiply connected shape containing four quantized vortices, as shown in Fig. 3(c). The four small skyrmions with $W = 1$ are then scattered in directions perpendicular to the incident directions. In this dynamics, the deviation of $W_{\rm tot}$ from 4 is less than 1%. After the scattering, we only observe skyrmions with $W = 1$; skyrmions with $W \geqslant 2$ are never produced. This is probably because the energy of n skyrmions with $W = 1$ is less than that of a single skyrmion with $W = n$.

Figure 4 shows the collision of two skyrmions with various winding numbers. In Fig. 4(a), two skyrmions with $W = 3$ ($W_{\rm tot} = 3 + 3 = 6$) collide with each other, and six skyrmions with unit winding number are scattered after the collision, which is similar to the dynamics in Figs. 2 and 3. Figure 4(b)

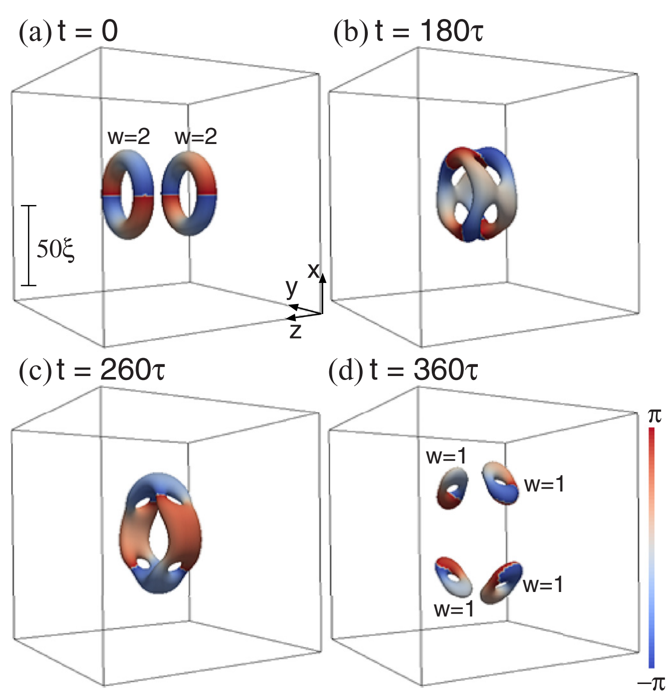

FIG. 3. Isodensity surfaces of component 1; the color represents the phase at the surface. Each skyrmion in (a) has winding number 2 ($n = \pm 2$ and $\ell = \pm 1$), and the total winding number is $W_{\rm tot} = 4$. Other conditions are the same as those in Fig. 2. See Ref. [43] for a movie of the dynamics.

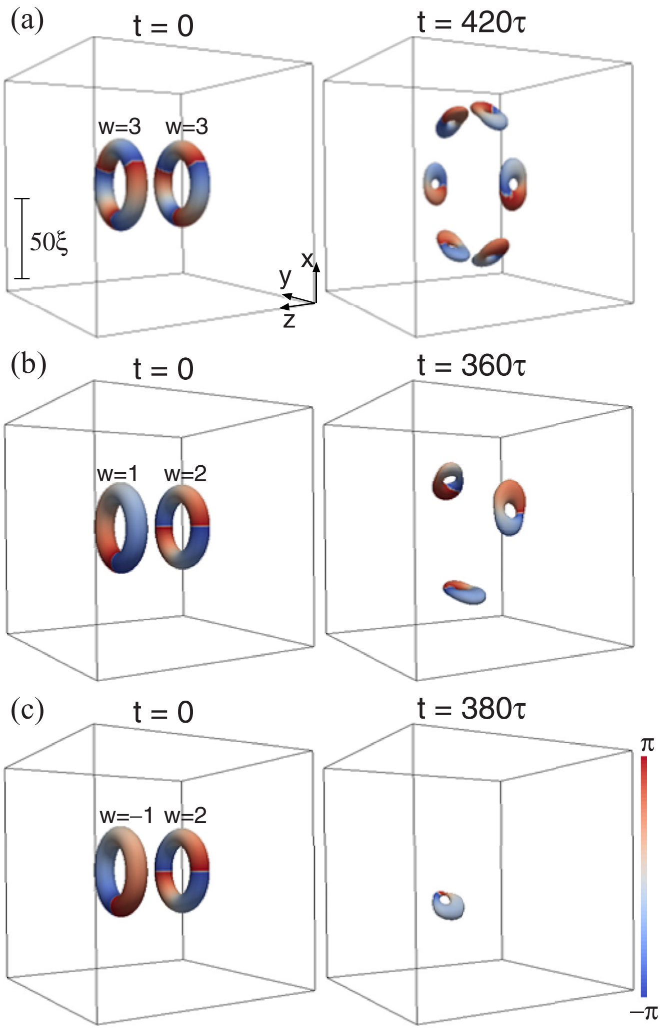

FIG. 4. Isodensity surfaces of component 1; the color represents the phase at the surface. The initial states of two skyrmions and the states after their collision are shown. (a) Winding numbers are 3 and 3 ($W_{\text{tot}} = 6$). (b) Winding numbers are 1 and 2 ($W_{\text{tot}} = 3$). (c) Winding numbers are −1 and 2 ($W_{\text{tot}} = 1$). Other conditions are the same as those in Fig. 2. All the skyrmions in the right-hand panels have unit winding number. See Ref. [43] for a movie of the dynamics.

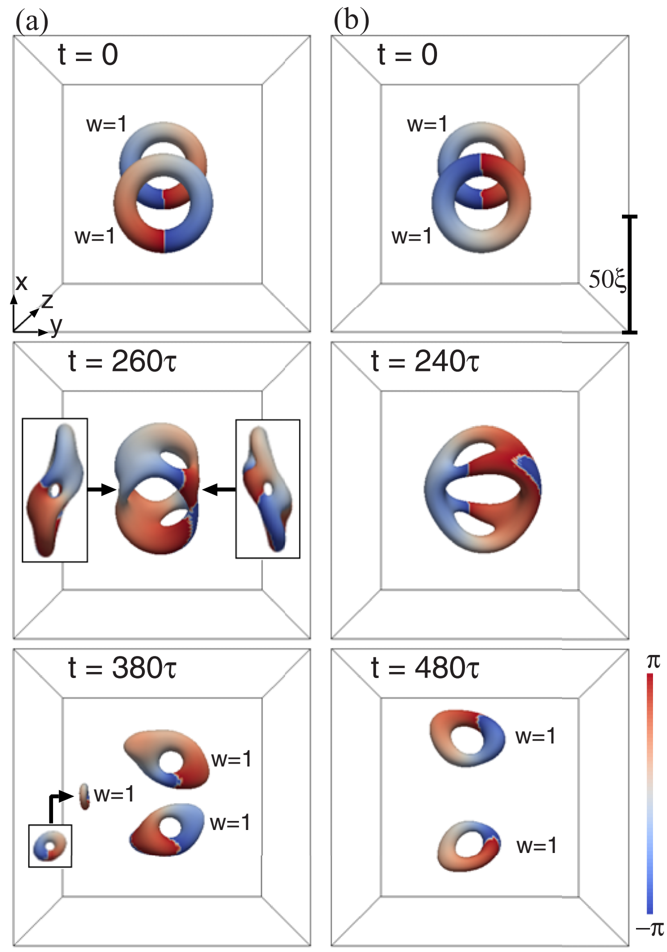

FIG. 5. Dynamics of off-axis collisions of skyrmions with $W = 1$ ($W_{\text{tot}} = 2$) and $\boldsymbol{r}_0 = (\pm 10\xi, 0, \pm 20\xi)$ (the impact parameter is 20ξ). Isodensity surfaces of component 1 are shown; the color represents the phase at the surface. The initial phase differences between the two donut-shaped components are (a) 0 and (b) π. Other conditions are the same as those in Fig. 2. See Ref. [43] for a movie of the dynamics.

shows the case of skyrmions with different winding numbers, $W = 1$ and $W = 2$ ($W_{\text{tot}} = 3$). After the collision, the three skyrmions with unit winding number are scattered. Figure 4(c) shows the case with $W = -1$ and $W = 2$. Since the total winding number is $W_{\text{tot}} = 1$, only a single small skyrmion with unit winding number is left after the collision, where most of component 1 has spread into component 2 without topological structure. We also found that a head-on collision between two skyrmions with $W_{\text{tot}} = 0$ (for example, $W = -1$ and $W = 1$) generates no topological structure, and component 1 spreads into component 2 after the collision (data not shown).

Figure 5 shows the dynamics of off-axis collisions of skyrmions with $W = 1$, where the impact parameter is 20ξ. The difference between Figs. 5(a) and 5(b) is only the initial phase of component 1: component 1 contained in the one skyrmion is multiplied by $e^{i\eta}$ with $\eta = \pi$ in Fig. 5(b). When the two donut shapes touch each other in Fig. 5(a), four quantized vortices are created between them ($t = 260\tau$). One of these decreases the winding number by 1, and the remaining three vortices increase the winding number by 3; thus, the total winding number remains $W_{\text{tot}} = 3 - 1 = 2$. As they split into skyrmions with $W = \pm 1$, the one with $W = -1$ (corresponding to the vortex in the right-hand inset) disappears; this increases the total winding number by 1, giving $W_{\text{tot}} = 3$ ($t = 380\tau$). The nonconservation of the total winding number indicates that the total density vanishes at some point, at which the wave function deviates from the SU(2) manifold. In Fig. 5(b), one of the initial donuts of component 1 is multiplied by $e^{i\eta} = e^{i\pi}$. In this case, two quantized vortices are created when the two donuts unite ($t = 240\tau$), and they are scattered as two skyrmions with $W = 1$ ($t = 480\tau$). The total winding number $W_{\text{tot}} = 2$ is conserved for the dynamics in Fig. 5(b).

Thus, the collision dynamics of skyrmions with a finite impact parameter depends on the initial relative phase η between the two donuts of component 1. We also found that the same is true for the oblique collisions. However, for head-on collisions as in Figs. 2–4, the initial relative phase η is not important, since it is described by $e^{iL_z\eta/W_{\rm tot}}\Psi$, where L_z is the z component of the angular momentum operator. Therefore, when $\eta \neq 0$, the entire dynamics is rotated around the z axis.

We have considered so far the case of $g_{11} = g_{22} = g_{12}$. For a more specific example, we consider $|F = 1, m_F = 1\rangle$ and $|F = 1, m_F = -1\rangle$ states of alkali-metal atoms. In this case, $g_{11} = g_{22} \equiv g$, and the two components are miscible ($g_{12}/g \simeq 0.97$) for ^{23}Na atoms and immiscible ($g_{12}/g \simeq 1.01$) for ^{87}Rb atoms. Using these parameters, we performed numerical simulations of skyrmion collisions and found that the dynamics are qualitatively the same as those for $g_{11} = g_{22} = g_{12}$. However, in a strongly immiscible case with $g_{12}/g \simeq 1.1$, we found that the total winding number is not conserved during collisions, which may be due to the large interface tension. For example, for $W_{\rm tot} = 2 + 2 = 4$, the four quantized vortices as shown in Fig. 3(c) escape from component 1, which is followed by the scattering of four objects without topological structures.

IV. CONCLUSIONS

We have numerically investigated the dynamics of collision and scattering of skyrmions in a two-component BEC. A skyrmion in a two-component BEC is composed of a quantized vortex ring in one component, whose donut-shaped core is occupied by a quantized vortex of the other component. Since a vortex ring has a momentum, a skyrmion travels at a constant velocity, as shown in Fig. 1. When two skyrmions are prepared and collide with each other, various dynamics can be observed; these depend on the winding numbers, impact parameters, collision angles, and phase differences. When two skyrmions, which both have $W = 1$, collide, they first merge into a skyrmion with $W_{\rm tot} = 2$, and then separate into two skyrmions with $W = 1$ and 1 and are scattered (Fig. 2). The scattering of skyrmions with unit winding number occurs even for a collision with $W = 2$ and 2. In this case, four skyrmions with unit winding number are scattered after the collision (Fig. 3). Similar dynamics are also observed for $W_{\rm tot} = 3 + 3$, $W_{\rm tot} = 1 + 2$, and $W_{\rm tot} = -1 + 2$ collisions, where, respectively, 6, 3, and 1 skyrmion(s) with unit winding number are scattered (Fig. 4). These dynamics imply that $W_{\rm tot}$ skyrmions with unit winding number are always scattered following head-on collisions in which the total winding number is conserved. For off-axis collisions, the dynamics depends on the relative phase of the two skyrmions (Fig. 5).

The dynamics of skyrmions studied in this paper can be reproduced experimentally, if skyrmions are created in a sufficiently large BEC in a controlled manner. Dynamical creation of skyrmions in a two-component BEC has been proposed in Refs. [29,44]. Once two skyrmions are created, their trajectories may be controllable by external potentials [13], which would enable us to collide skyrmions at the desired angle and with the desired impact parameter.

ACKNOWLEDGMENTS

We thank Y. Kawaguchi for fruitful discussion. This work was supported by JSPS KAKENHI Grant No. 26400414 and by MEXT KAKENHI Grant No. 25103007.

[1] T. H. R. Skyrme, Proc. R. Soc. London A **260**, 127 (1961); Nucl. Phys. **31**, 556 (1962).
[2] J. R. Kirtley, C. C. Tsuei, M. Rupp, J. Z. Sun, L. S. Yu-Jahnes, A. Gupta, M. B. Ketchen, K. A. Moler, and M. Bhushan, Phys. Rev. Lett. **76**, 1336 (1996).
[3] J. Jang, D. G. Ferguson, V. Vakaryuk, R. Budakian, S. B. Chung, P. M. Goldbart, and Y. Maeno, Science **331**, 186 (2011).
[4] S. Autti, V. V. Dmitriev, V. B. Eltsov, J. Mäkinen, G. E. Volovik, A. N. Yudin, and V. V. Zavjalov, arXiv:1508.02197.
[5] L. S. Leslie, A. Hansen, K. C. Wright, B. M. Deutsch, and N. P. Bigelow, Phys. Rev. Lett. **103**, 250401 (2009).
[6] J. Y. Choi, W. J. Kwon, and Y.-I. Shin, Phys. Rev. Lett. **108**, 035301 (2012).
[7] M. W. Ray, E. Ruokokoski, S. Kandel, M. Möttönen, and D. S. Hall, Nature (London) **505**, 657 (2014).
[8] M. W. Ray, E. Ruokokoski, K. Tiurev, M. Möttönen, and D. S. Hall, Science **348**, 544 (2015).
[9] S. W. Seo, S. Kang, W. J. Kwon, and Y.-I. Shin, Phys. Rev. Lett. **115**, 015301 (2015).
[10] K. G. Lagoudakis, T. Ostatnický, A. V. Kavokin, Y. G. Rubo, R. André, and B. Deveaued-Plédran, Science **326**, 974 (2009).
[11] R. Hivet, H. Flayac, D. D. Solnyshkov, D. Tanese, T. Boulier, D. Andreoli, E. Giacobino, J. Bloch, A. Bramatik, G. Malpuech, and A. Amo, Nat. Phys. **8**, 724 (2012).
[12] T. Frisch, Y. Pomeau, and S. Rica, Phys. Rev. Lett. **69**, 1644 (1992).
[13] T. Aioi, T. Kadokura, T. Kishimoto, and H. Saito, Phys. Rev. X **1**, 021003 (2011).
[14] S. Inouye, S. Gupta, T. Rosenband, A. P. Chikkatur, A. Görlitz, T. L. Gustavson, A. E. Leanhardt, D. E. Pritchard, and W. Ketterle, Phys. Rev. Lett. **87**, 080402 (2001).
[15] T. W. Neely, E. C. Samson, A. S. Bradley, M. J. Davis, and B. P. Anderson, Phys. Rev. Lett. **104**, 160401 (2010).
[16] D. V. Freilich, D. M. Bianchi, A. M. Kaufman, T. K. Langin, and D. S. Hall, Science **329**, 1182 (2010).
[17] W. J. Kwon, S. W. Seo, and Y.-I. Shin, Phys. Rev. A **92**, 033613 (2015).
[18] K. Sasaki, N. Suzuki, and H. Saito, Phys. Rev. Lett. **104**, 150404 (2010).
[19] R. Navarro, R. Carretero-González, P. J. Torres, P. G. Kevrekidis, D. J. Frantzeskakis, M. W. Ray, E. Altuntaş, and D. S. Hall, Phys. Rev. Lett. **110**, 225301 (2013).
[20] S. Serafini, M. Barbiero, M. Debortoli, S. Donadello, F. Larcher, F. Dalfovo, G. Lamporesi, and G. Ferrari, Phys. Rev. Lett. **115**, 170402 (2015).
[21] K. W. Schwarz, Phys. Rev. B **31**, 5782 (1985).
[22] J. Koplik and H. Levine, Phys. Rev. Lett. **71**, 1375 (1993).
[23] K. Sasaki, N. Suzuki, and H. Saito, Phys. Rev. A **83**, 033602 (2011).
[24] R. M. Caplan, J. D. Talley, R. Carretero-González, and P. G. Kevrekidis, Phys. Fluids **26**, 097101 (2014).
[25] J. Koplik and H. Levine, Phys. Rev. Lett. **76**, 4745 (1996).

[26] M. Eto, K. Kasamatsu, M. Nitta, H. Takeuchi, and M. Tsubota, Phys. Rev. A **83**, 063603 (2011).
[27] M. Kobayashi, Y. Kawaguchi, M. Nitta, and M. Ueda, Phys. Rev. Lett. **103**, 115301 (2009).
[28] T. Kaneda and H. Saito, Phys. Rev. A **90**, 053632 (2014).
[29] K. Sasaki, N. Suzuki, and H. Saito, Phys. Rev. A **83**, 053606 (2011).
[30] S. W. Seo, W. J. Kwon, S. Kang, and Y.-I. Shin, arXiv:1512.07696.
[31] A. E. Allder, S. E. Koonin, R. Seki, and H. M. Sommermann, Phys. Rev. Lett. **59**, 2836 (1987).
[32] R. A. Battye and P. M. Sutcliffe, Phys. Lett. B **391**, 150 (1997).
[33] D. Foster and S. Krusch, Nucl. Phys. B **897**, 697 (2015).
[34] I. F. Herbut and M. Oshikawa, Phys. Rev. Lett. **97**, 080403 (2006).
[35] S. Wüster, T. E. Argue, and C. M. Savage, Phys. Rev. A **72**, 043616 (2005).
[36] J. Ruostekoski and J. R. Anglin, Phys. Rev. Lett. **86**, 3934 (2001).
[37] U. Al Khawaja and H. Stoof, Nature (London) **411**, 918 (2001); Phys. Rev. A **64**, 043612 (2001).
[38] R. A. Battye, N. R. Cooper, and P. M. Sutcliffe, Phys. Rev. Lett. **88**, 080401 (2002).
[39] C. M. Savage and J. Ruostekoski, Phys. Rev. Lett. **91**, 010403 (2003).
[40] J. Ruostekoski, Phys. Rev. A **70**, 041601(R) (2004).
[41] Although a skyrmion ground state does not exist for $g_{11} = g_{22} = g_{12}$ [38], there exists a stable stationary state traveling at a constant velocity.
[42] A. L. Fetter, Phys. Rev. **151**, 100 (1966).
[43] See Supplemental Material at http://link.aps.org/supplemental/10.1103/PhysRevA.93.033611 for movies of the skyrmion dynamics.
[44] M. Nitta, K. Kasamatsu, M. Tsubota, and H. Takeuchi, Phys. Rev. A **85**, 053639 (2012).